

Binary neutron star mergers & multimessenger signals

INT@UW, Seattle, WA

Steve Liebling

With:

Matt Anderson (IU) Liliana Caballero (U.Guelph) Luis Lehner (Perimeter) David Neilsen (BYU) Patrick Motl (IU) Evan O'Connor (NCSU) Carlos Palenzuela (UIB)

Long Island University, New York, USA

August 15, 2017



Physics Motivation

- Examine effects of EOS in various scenarios, notably BNS mergers
- Study EM Events: sGRBs, **kilonovae/r-process**, FRBs
- LIGO:
 - Look for EM precursors
 - Localization via EM signals
 - Multimessenger astronomy (e.g. neutrinos if very close)
 - Fully nonlinear tidal effects
 - Tests of GR:
 - alternative gravity
 - differentiate from exotic matter (boson stars)
 - dark matter

Our Evolution Code: Fluid

[Palenzuela,SLL,Neilsen,Lehner,Caballero,O'Connor,Anderson,1505.01607]

[Neilsen,SLL,Anderson,Lehner,O'Connor,Palenzuela,1403.3680]

- Barytropic, finite-temperature EOS
- EOS used are constrained by the most massive observed NSs
- Involves temperature and composition (electron fraction)
- MHD HRSC
- Adapts open-source neutrino leakage code from stellarcollapse.org
- Implements novel, local calculation of optical depth which tracks binary NS

Our Evolution Code: Other

[Palenzuela,SLL,Neilsen,Lehner,Caballero,O'Connor,Anderson,1505.01607]

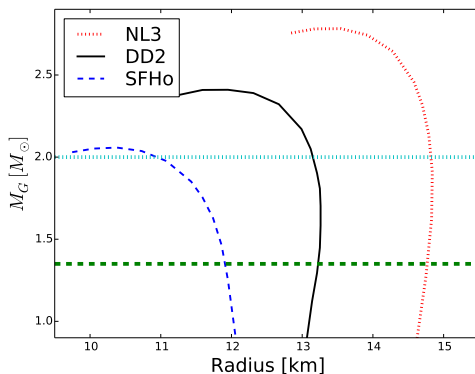
[Neilsen,SLL,Anderson,Lehner,O'Connor,Palenzuela,1403.3680]

- HAD
- Distributed
- Fully nonlinear GR (BSSN scheme)
- AMR with subcycling in time
- GR wave extraction
- Tracers (simply advected or geodesic)

Choice of Realistic, microphysical EoS

Choose range of EoS that satisfy observational constraint:

- NLS—stiff—large radii
- DD2—moderate—intermediate radii
- SFHo—soft—small radii

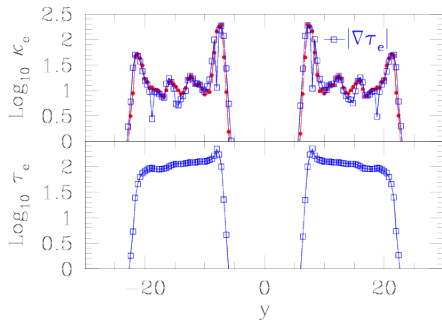


Initial Data

- Use LORENE package to generate binaries in quasi-circular orbits
- Total mass $2.7M_{\odot}$
- 45 km initial separation...4-5 orbits prior to merger
- Finest resolution: 230 meters in neighborhood of each star

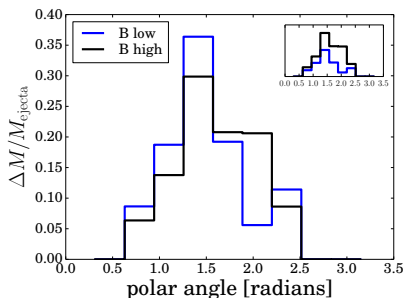
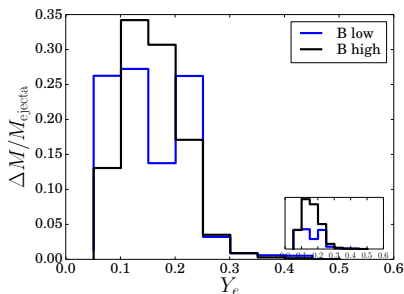
EoS	q	ν	$m_b^{(1)}, m_g^{(1)}$ [M_{\odot}]	$m_b^{(2)}, m_g^{(2)}$ [M_{\odot}]	$R^{(1)}$ [km]	$R^{(2)}$ [km]	$C^{(1)}$	$C^{(2)}$	J_0^{ADM} [$G M_{\odot}^2/c$]	Ω_0 [rad/s]	f_0^{GW} [Hz]	M_{eject} [$10^{-3}M_{\odot}$]
NL3	1.0	0.250	1.47, 1.36	1.47, 1.36	14.80	14.80	0.136	0.136	7.40	1778	566	0.015
NL3	0.85	0.248	1.34, 1.25	1.60, 1.47	14.75	14.8	0.125	0.147	7.35	1777	566	2.3
DD2	1.0	0.250	1.49, 1.36	1.49, 1.36	13.22	13.22	0.152	0.152	7.39	1776	565	0.43
DD2	0.85	0.248	1.36, 1.29	1.62, 1.47	13.20	13.25	0.144	0.164	7.34	1775	565	0.42
DD2	0.76	0.245	1.27, 1.18	1.71, 1.54	13.16	13.25	0.132	0.172	7.26	1775	565	1.3
SFHo	1.0	0.250	1.50, 1.36	1.50, 1.36	11.90	11.90	0.169	0.169	7.38	1775	565	3.4
SFHo	0.85	0.248	1.37, 1.25	1.63, 1.47	11.95	11.85	0.154	0.183	7.31	1773	564	2.2

Novel Optical Depth Calculation [PRD 1403.3680]



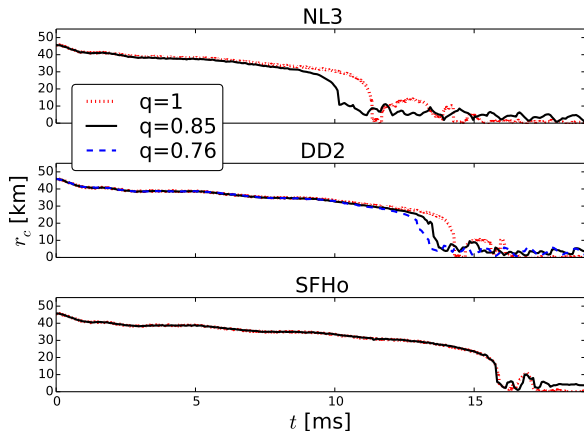
- conventional to shoot rays and integrate opacity, but non-local, somewhat arbitrary which rays to consider
- instead at each point (i) start with minimum depth of neighbor, (ii) add depth to get to neighbor
- easy, works well, tracks binaries, gradient matches opacity

Magnetic Effects [PRD 1505.01607]



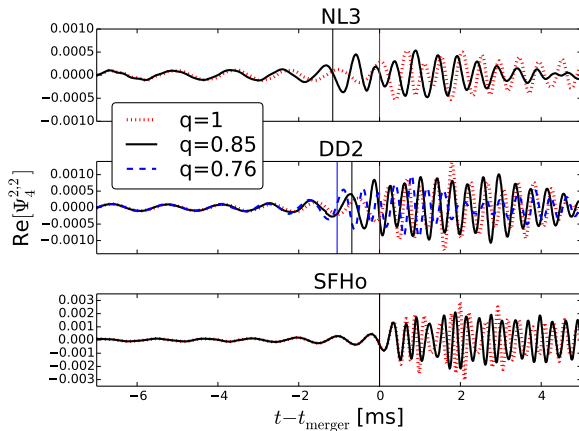
- DD2; magnetic dipole; “effective driver” for subgrid instabilities [Giacomazzo+ 1410.0013] $10^{13} \rightarrow 10^{16}$ G
- Dynamics largely the same with subgrid model “on”
- However, subgrid model causes: (i) twice material ejected (magnetic pressure) (ii) less flat Y_e distribution (iii) additional extra material mostly equatorial

Separation



- $q = 1$ corresponds to equal mass case
- unequal cases merge earlier than equal
- smaller (radius) stars less sensitive to mass ratio

Waveforms

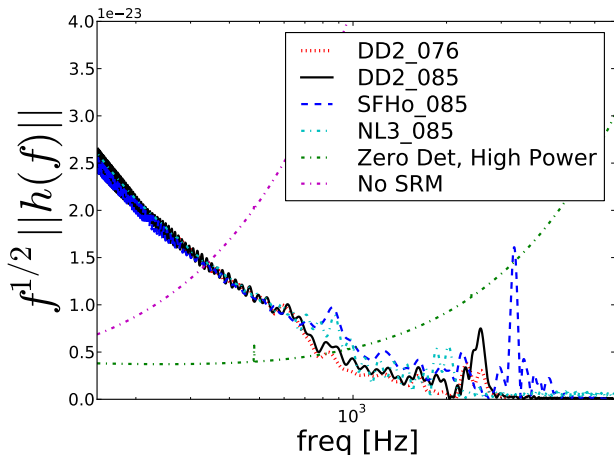


- $t = 0$ corresponds to first contact for $q = 1$ binary

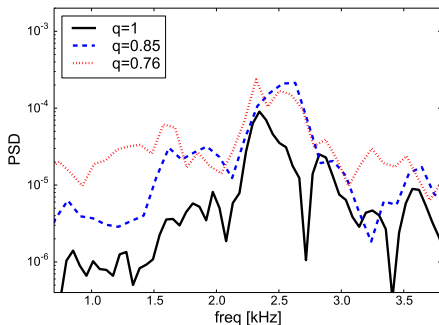
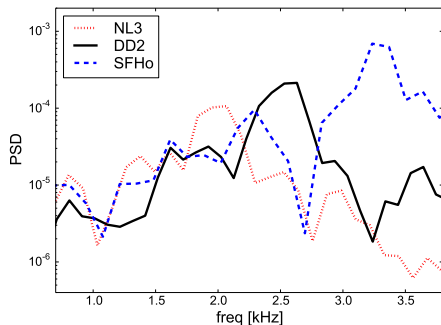
- times of contact for unequal cases shown w/ vertical lines

Could aLIGO differentiate among EOS?

Best case scenario (“Zero Detuned, High Power”) configuration of aLIGO could differentiate among stiffest and softest EOS at 100 Mpc



Post-Merger GW Power Spectral Densities



- Spectra characterized by various peaks differing among EOS
- Dominant f_{peak} associated with rotation and quadrupolar structure
- Using language of [Bauswein, Stergioulas, PRD'15]
- Peak frequencies agree within 5% with similar mass ratios of [Bernuzzi, Dietrich, Nagar PRL'15]

Post-Merger GW Frequencies

Table 2. Prominent oscillation frequencies (kHz) in the power spectral densities of the post-merger gravitational waveform compared with predicted values.

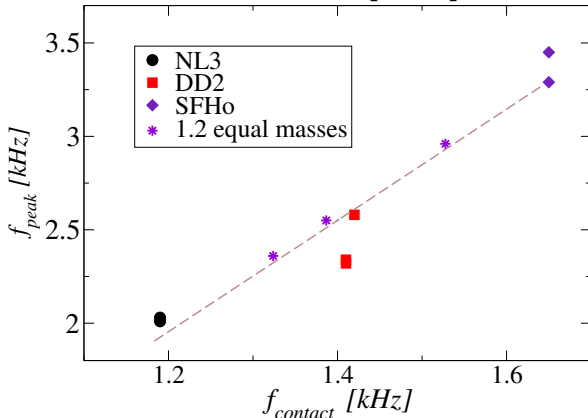
EoS	q	f_1	f_2	f_3	f_4	f_{peak}	f_{spiral}	$f_2 - 0$	f_c
NL3	1.0	2.03	1.54	0.83	—	2.2	1.6	1.2	1.19
NL3	0.85	2.01	1.61	1.37	0.8	—	—	—	1.19
DD2	1.0	2.34	1.97	1.82	1.62	2.6	1.9	1.5	1.41
DD2	0.85	2.58	1.92	1.62	—	—	—	—	1.42
DD2	0.76	2.32	1.86	1.62	—	—	—	—	1.41
SFHo	1.0	3.45	2.59	2.20	1.62	3.2	2.4	2.1	1.65
SFHo	0.85	3.29	2.29	1.61	—	—	—	—	1.65

Note. The frequencies f_1 , f_2 , f_3 , and f_4 . Correspond to various peaks of the post-merger GW spectrum (see figure 3). f_{peak} and f_{spiral} are the predicted peak frequencies from [48]. The correspondence between f_1 and f_{peak} , f_2 and f_{spiral} , and either f_3 or f_4 with $f_2 - 0$ suggests consistency with the model presented in [48] (which was tailored for the equal mass case, but reports errors $< 5\%$ for mass ratios $q = 0.92$). f_c is the computed contact frequency (8).

Remnant's peak GW Frequency

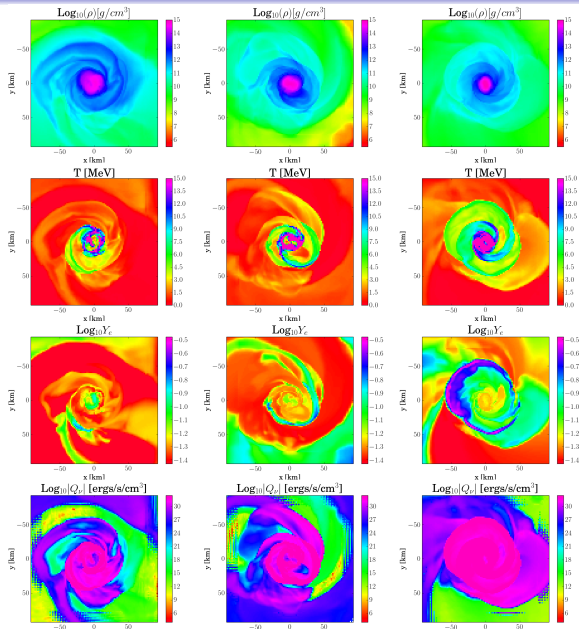
In terms of contact frequency: $f_c = \frac{1}{\pi M_g} \left(\frac{m_g^{(1)}}{M_g C_1} + \frac{m_g^{(2)}}{M_g C_2} \right)^{-3/2}$

yields fit: $f_{\text{peak}} [\text{kHz}] = -1.61 + 2.96 f_c \left[\frac{2.7 M_\odot}{M} \right] [\text{kHz}]$



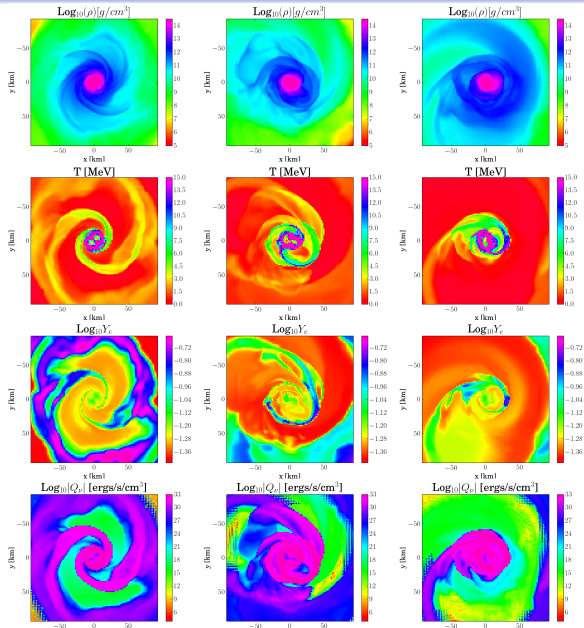
NL3 (left),
DD2 (middle),
SFHo (right) for
 $q = 0.85$ 3ms
after merger

- SFHo remnant more centrally condensed and hotter
- SFHo also drives decompression of hot material to lower densities where positron capture raises electron fraction



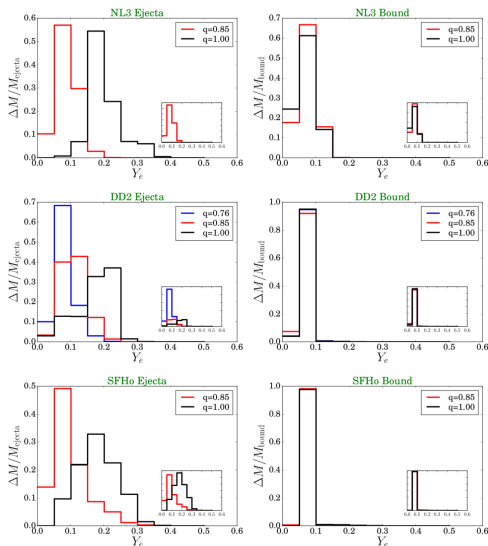
DD2, $q = 1$ (left),
 $q = 0.85$ (middle),
 $q = 0.75$ (right)

- Decreased electron fraction in unequal cases—tidal ejecta
- Spiral arm apparent in unequal cases



Ejecta Properties: Electron Fraction

- Amount of ejecta increases with mass ratio
- Electron Fraction decreases with mass ratio
- As mass ratio decreases, ejected material is cooler, dominated by neutron-rich, tidal tail material
- Lower temperature inhibits positron production and neutron capture... Y_e similar to original NS material



Estimates of possible EM signals

Kilonova: [Barnes, Kasen, 2013]

$$t_{\text{peak}}^k \approx 0.25 \text{ days} \left[\frac{M_{\text{eject}}}{10^{-2} M_{\odot}} \right]^{1/2} \left[\frac{v}{0.3c} \right]^{-1/2}$$

$$L \approx 2 \times 10^{41} \text{ erg/s} \left[\frac{M_{\text{eject}}}{10^{-2} M_{\odot}} \right]^{1/2} \left[\frac{v}{0.3c} \right]^{1/2}$$

Radio emission from collision with ISM: [Nakar, Piran, 2011]

$$t_{\text{peak}} \approx 6 \text{ yr} \left[\frac{E_{\text{kin}}}{10^{51} \text{ erg}} \right]^{1/3} \left[\frac{n_0}{0.1 \text{ cm}^{-3}} \right]^{-1/3} \left[\frac{v}{0.3c} \right]^{-5/3}$$

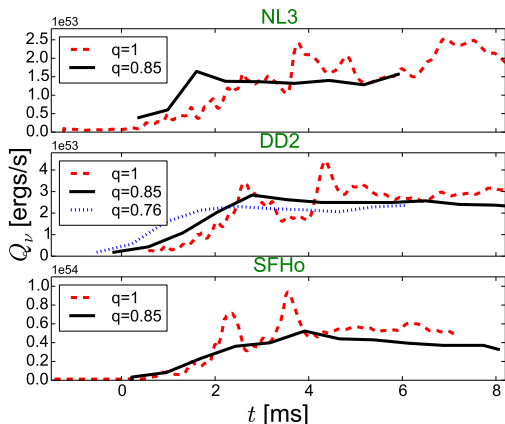
$F(\nu_{\text{obs}}) \approx$

$$0.6 \text{ mJy} \left[\frac{E_{\text{kin}}}{10^{51} \text{ erg}} \right] \left[\frac{n_0}{0.1 \text{ cm}^{-3}} \right]^{7/8} \left[\frac{v}{0.3c} \right]^{11/4} \left[\frac{\nu_{\text{obs}}}{1 \text{ GHz}} \right]^{-3/4} \left[\frac{d}{100 \text{ Mpc}} \right]^{-2}$$

EoS	q	$L [10^{40} \text{ erg/s}]$	t_{peak}^k [days]	$M_{\text{eject}} [10^{-3} M_{\odot}]$	v/c	$E_{\text{kin}} [10^{50} \text{ ergs}]$	t_{peak} [yr]	$F(1 \text{ GHz})$ [mJy]
NL3	1.0	0.9	0.008	0.015	0.45	0.01	0.31	1.8×10^{-3}
NL3	0.85	8.8	0.13	2.3	0.25	1.22	4.0	4.4×10^{-2}
DD2	1.0	4.1	0.05	0.43	0.3	0.31	1.9	1.9×10^{-2}
DD2	0.85	4.1	0.05	0.42	0.3	0.29	1.8	1.7×10^{-2}
DD2	0.76	7.2	0.09	1.3	0.3	0.76	2.5	4.6×10^{-2}
SFH _o	1.0	10.6	0.16	3.4	0.25	1.8	4.6	6.5×10^{-2}
SFH _o	0.85	8.6	0.13	2.2	0.25	1.8	4.6	6.5×10^{-2}

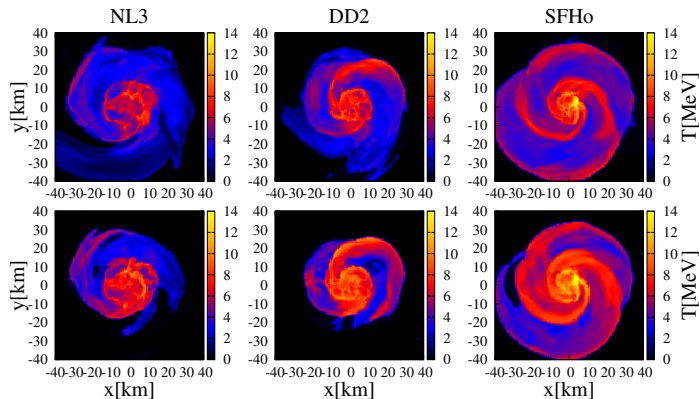
Neutrino Emission

- Softest EoS most luminous and highest average neutrino energies for any mass ratio because highest temperature



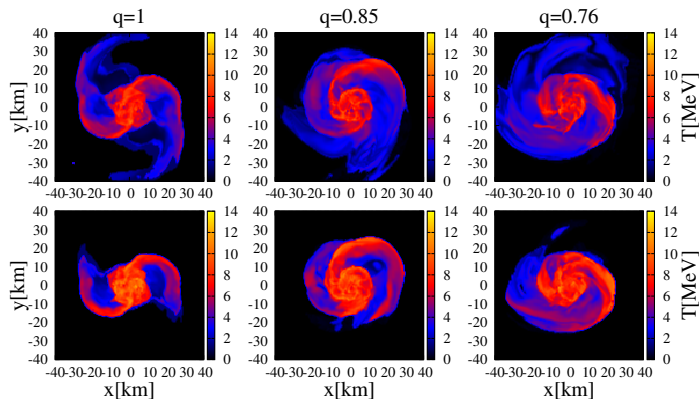
Neutrino Analysis via (post-processed) ray tracing

$q = 0.85$ **Top:** electron neutrino surface **Bottom:** electron antineutrino surface



Neutrino Analysis via (post-processed) ray tracing

DD2 **Top:** electron neutrino surface **Bottom:** electron antineutrino surface



Neutrino Emission: Detectability

Assume 10kpc distant in SuperKamiokande-like water Cherenkov detector

EoS	q	t [ms]	$\langle E_{\bar{\nu}_e} \rangle$ [MeV]	$\langle E_{\nu_e} \rangle$ [MeV]	$L_{\bar{\nu}_e}$ [10^{53} erg/s]	R_ν [#/ms]
NL3	1.0	3.4	18.5 (22.4)	15.2 (18.3)	0.7	18
NL3	0.85	3.0	15.6 (18.7)	12.6 (15.1)	0.8	18
DD2	1.0	3.3	18.3 (22.1)	14.6 (17.4)	1.1	28
DD2	0.85	2.8	18.1 (21.7)	15.1 (18.0)	1.0	25
DD2	0.76	2.4	19.7 (23.9)	14.8 (17.9)	1.3	36
SFHo	1.0	3.5	24.6 (29.7)	23.5 (28.3)	3.5	121
SFHo	0.85	3.9	17.8 (21.3)	15.3 (17.9)	2.0	50

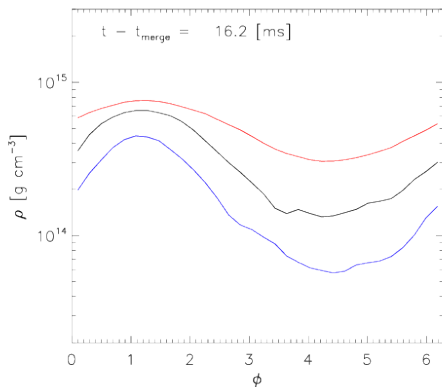
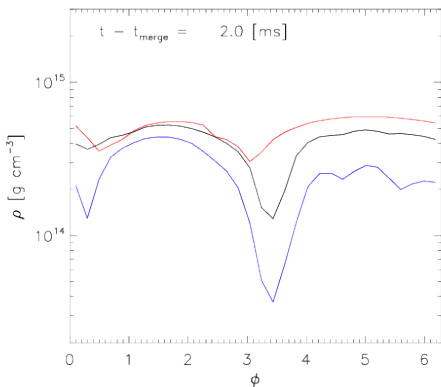
BNS Conclusions

- GW:
 - Peak frequency of remnant can be estimated via a fit based on the contact frequency
 - Stiffer EoS more sensitive to mass ratio because larger radius
- Ejecta:
 - Decreasing mass ratio makes kilonova more likely
 - Obtaining individual masses from GW would benefit EM observations
 - Neutron rich ejecta...peaked around 0.2
 - promising for r-process IR afterglow
(recent observation SGRB 130603B [Tanvir, et al, Nature, 2013] and [Berger, et al, ApJ, 2013])
- Neutrino Emission:
 - Soft EOS more luminous
 - Smaller mass ratios result in more dispersed neutrino surfaces, smaller max temps

The $m = 1$ Instability

- The $l = 2$ $m = 2$ mode dominates the GW signal of BNS mergers,
- The weaker $l = 2$ $m = 1$ mode develops via a recently noticed instability
 - Newtonian simulations of [Ou, Tohline, ApJ'06]
 - Seen more recently in [Corvino+, CQG'10]
[Dietrick+, PRD'15] [East+, PRD'16] [Radice+, PRD'16]
- “Benefits”:
 - Occurs at half the frequency of dominant mode where noise is less
 - Lasts longer because less damped: (i) less GW radiative (ii) instabilities driving it
 - Occurs postmerger, and be specifically targeted in time and frequency

$m = 2$ develops into $m = 1$ for $q = 0.85$ DD2

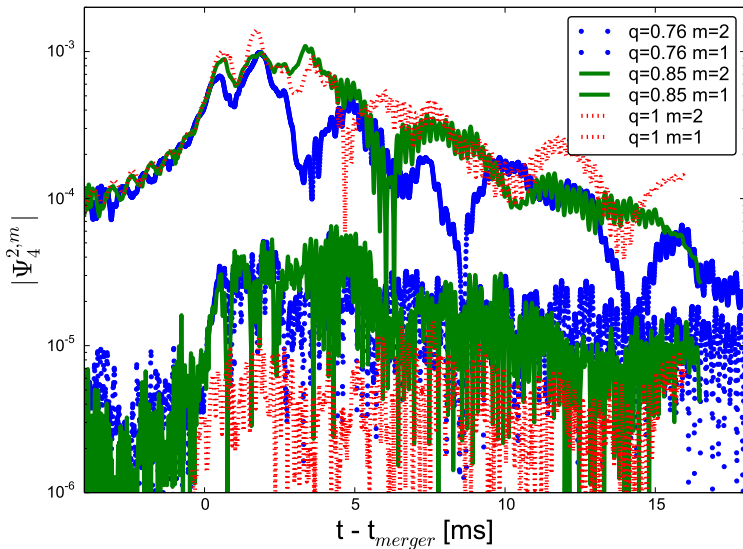


- colors indicate increasing radii (red-black-blue)
- average mass density on equatorial plane

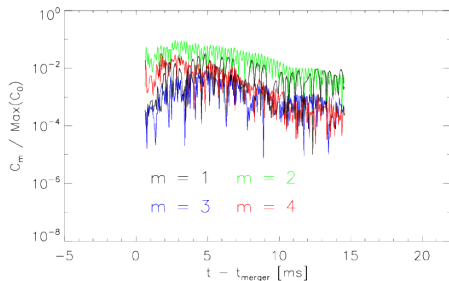
See also

[East, Paschalidis, Pretorius, Shapiro, 1511.01093]

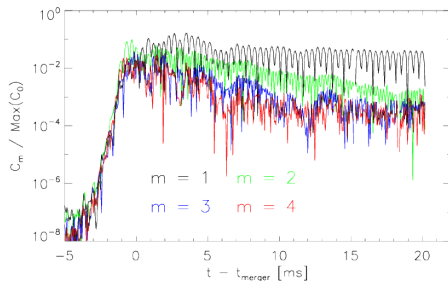
and [Radice, Bernuzzi, Ott, 1603.05726]

Growth of $m = 1$ Mode in GW Signal for DD2

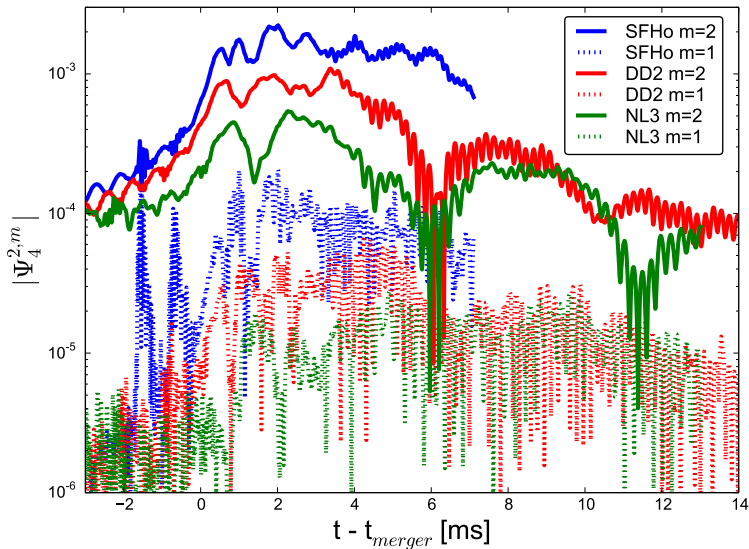
Density Decomposition into Azimuthal Modes for DD2



$q = 1$



$q = 0.76$

Effect of EoS on $m = 1$ mode instability

Detectability

Using:

$$\rho^2 \simeq \frac{2}{S_n(f)} \int_0^T h^2 dt$$

We arrive at

$$\rho_{m=1} \approx 11 \times \left[\frac{6 \times 10^{-24} \text{Hz}^{-1/2}}{\sqrt{S_n(f_{m1})}} \right] \left[\frac{|\Psi_{4m=1}^0|}{5 \times 10^{-5}} \right] \left[\frac{1.3 \text{kHz}}{f_{m1}} \right]^2 \left[\frac{T}{10 \text{ms}} \right]^{1/2} \left[\frac{10 \text{Mpc}}{L} \right]$$

Not particularly encouraging, but...

Detectability

- The $m = 1$ mode **lasts longer** than the $m = 2$ mode
- Occurs at **low frequency** and hence in more sensitive region of LIGO's noise curve
- Its frequency is precisely half that of the $m = 2$ and can therefore be **explicitly targeted**
- Could benefit from BNS mode stacking [Yang+, '17]
[Bose+, '17]

for sub-threshold SNR of unity, reach to 100 Mpc to see $m = 1$ mode

Provides another avenue for extracting information about the equation of state

- Weaker for stiff EoS than for soft EoS
- For smaller mass ratios, $m = 1$ becomes stronger and saturates earlier